

## Heme d<sub>1</sub> Nitrosyl Complex of cd<sub>1</sub> Nitrite Reductase Studied by High-Field-Pulse Electron Paramagnetic Resonance Spectroscopy

Marina Radoul,<sup>†</sup> Fabio Centola,<sup>‡</sup> Serena Rinaldo,<sup>‡</sup> Francesca Cutruzzolà,<sup>‡</sup> Israel Pecht,<sup>§</sup> and Daniella Goldfarb<sup>\*†</sup>

Departments of Chemical Physics and Immunology, Weizmann Institute of Science, Rehovot 76100, Israel, and Dipartimento di Scienze Biochimiche, “A. Rossi Fanelli” and Istituto di Biologia e Patologia Molecolari del CNR, Università di Roma “La Sapienza”, Rome, Italy

Received December 9, 2008

W-band (95 GHz) HYSCORE and pulse ENDOR are used to characterize the nitrosyl d<sub>1</sub> heme complex (d<sub>1</sub>NO) of cd<sub>1</sub> nitrite reductase from *Pseudomonas aeruginosa* in the wild type and the Y10F mutant. The spectra and the derived <sup>14</sup>N hyperfine and quadrupole interactions were found to be the same for wt and Y10F. This suggests that Tyr10 does not influence the NO ligand orientation in the reduced state in solution. This study is the first application of HYSCORE at high fields and shows its potential for characterizing low  $\gamma$  nuclei with large hyperfine couplings.

cd<sub>1</sub> nitrite reductase (cd<sub>1</sub> NiR) catalyzes the one-electron reduction of nitrite (NO<sub>2</sub><sup>-</sup>) to nitric oxide (NO).<sup>1</sup> The enzyme is a homodimer; each monomer contains a c-type heme that acts as the electron mediator from the reducing substrate and a d<sub>1</sub>-type heme that provides the nitrite binding and reduction site. The enzymatic reaction is intriguing because it involves the reduction of an electron-rich species, i.e., the nitrite anion, possibly followed by protonation and dehydration.<sup>2</sup> More importantly, product inhibition may occur because NO has been assumed to form a stable complex with Fe<sup>II</sup> d<sub>1</sub> heme (d<sub>1</sub>NO).<sup>3</sup> The product dissociation mechanism is therefore important, and a recent report has shown that NO dissociation from the Fe<sup>II</sup> d<sub>1</sub> heme may indeed occur rapidly, a property that is unique to this unusual heme.<sup>2</sup> Although several rationales for the cd<sub>1</sub> NiR reaction pattern have been proposed, the evidence emerging from experiments employing cd<sub>1</sub> NiRs isolated from different sources still does not provide a consistent picture.<sup>4–6</sup>

NO binding to iron(II) hemes often forms distinct types of complexes. The electron paramagnetic resonance (EPR) spectrum of NO-bound iron(II) myoglobin (MbNO) reveals one complex with an axial *g* factor and another with a rhombic *g* factor<sup>7</sup>, and the relative population of the two types is temperature-dependent. The structure of the heme pocket affects the properties of the NO complexes and the equilibrium between them.<sup>8</sup> The low-temperature EPR spectrum of d<sub>1</sub>NO of the *Pseudomonas aeruginosa* (Pa) enzyme was found to be also buffer-dependent.<sup>9</sup>

To explore the effect of the amino acid residues in the distal pocket of the d<sub>1</sub> heme on the properties of the NO complex, we have studied d<sub>1</sub>NO formed by the wild type (wt) Pa enzyme and by its Y10F mutant in frozen solutions. The crystal structure of the wt enzyme shows that in the oxidized state Tyr10 forms a hydrogen bond with the OH ligand of the d<sub>1</sub> heme but not with the NO in the reduced NO-bound form.<sup>10,11</sup> The structure of the nitrosyl–heme complexes in solution may be different from that in the crystal; for example, the two forms appearing in frozen solutions of MbNO do not coexist in frozen crystals.<sup>12</sup>

So far the nitrosyl–heme complexes have been characterized primarily by continuous wave (cw) EPR, and by a few electron–nuclear double resonance (ENDOR) and hyperfine

\* To whom correspondence should be addressed. E-mail: daniella.goldfarb@weizmann.ac.il.

<sup>†</sup> Department of Chemical Physics, Weizmann Institute of Science.

<sup>‡</sup> Università di Roma “La Sapienza”.

<sup>§</sup> Department of Immunology, Weizmann Institute of Science.

(1) Zumft, W. G. *Microbiol. Mol. Biol. Rev.* **1997**, *61*, 533–616.

(2) Silvestrini, M. C.; Falcinelli, S.; Ciabatti, I.; Cutruzzolà, F.; Brunori, M. *Biochimie* **1994**, *76*, 641–654.

(3) Rinaldo, S.; Arcovito, A.; Brunori, M.; Cutruzzolà, F. *J. Biol. Chem.* **2007**, *282* (20), 14761–14767.

(4) Allen, J. W. A.; Barker, P. D.; Daltrop, O.; Stevens, J. M.; Tomlinson, E. J.; Sinha, N.; Sambongi, Y.; Ferguson, S. J. *Dalton Trans.* **2005**, *21*, 3410–3418.

(5) Cutruzzolà, F.; Brown, K.; Wilson, E.; Bellelli, A.; Arese, M.; Tegoni, M.; Cambillau, C.; Brunori, M. *Proc. Nat. Acad. Sci. U.S.A.* **2001**, *98*, 2232–2237.

(6) Zajicek, R. S.; Cartron, M. L.; Ferguson, J. S. *Biochemistry* **2006**, *45*, 11208–11216.

(7) Morse, R. H.; Chan, S. I. *J. Biol. Chem.* **1980**, *255*, 7876–7882.

(8) Van Doorslaer, S.; Vinck, E. *Phys. Chem. Chem. Phys.* **2007**, *9*, 4620–4638.

(9) Johnson, M. K.; Thomson, A. J.; Walsh, T. A.; Barber, D.; Greenwood, C. *Biochem. J.* **1980**, *189*, 285–294.

(10) Nurizzo, D.; Silvestrini, M. C.; Mathieu, M.; Cutruzzolà, F.; Bourgeois, D.; Fülöp, V.; Hajdu, J.; Brunori, M.; Tegoni, M.; Cambillau, C. *Structure* **1997**, *5*, 1157–1171.

(11) Nurizzo, D.; Cutruzzolà, F.; Arese, M.; Bourgeois, D.; Brunori, M.; Cambillau, C.; Tegoni, M. *Biochemistry* **1998**, *37*, 13987–13996.

(12) Copeland, D. M.; Soares, A. S.; West, A. H.; Richter-Addo, G. B. *J. Biol. Inorg. Chem.* **2006**, *100*, 1413–1425.

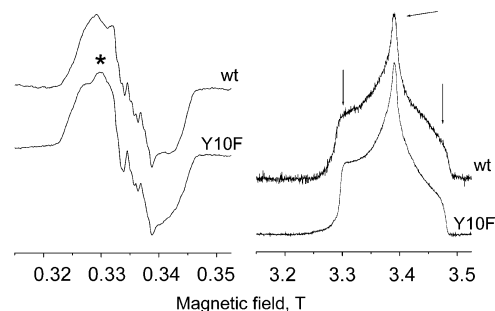


**Figure 1.** Spectra of  $d_1\text{NO}$  in wt and Y10F. (A) cw X-band EPR, 130 K; an asterisk marks the contribution of the axial form. (B) W-band two-pulse echo-detected EPR, 7 K. The pulse lengths were 100 and 200 ns, respectively, and the time interval was 600 ns. The arrows denote the positions where HYSCORE and ENDOR measurements were performed.

sublevel correlation (HYSCORE) spectroscopy at X-band frequencies ( $\sim 9.5$  GHz).<sup>13,14</sup> In the present study, we have used high-frequency, W-band (94.9 GHz) EPR, ENDOR, and HYSCORE in order to resolve the  $^{14}\text{N}$  hyperfine and quadrupolar interactions of the proximal histidine,  $^{14}\text{N}(\text{His})$ , and  $^{14}\text{N}$  of  $d_1\text{NO}$  in wt and its Y10F mutant.

wt  $\text{cd}_1\text{NiR}$  and Y10F were purified and prepared according to procedures described earlier.<sup>15,16</sup>  $d_1\text{NO}$  was prepared under anaerobic conditions in a 50 mM sodium phosphate buffer at pH 8.0, where NO binds only to the  $\text{Fe}^{\text{II}}$   $d_1$  heme.<sup>17</sup> The enzyme was reduced with an excess ( $\sim 200$ -fold) of sodium ascorbate, and after approximately 1 h, sodium nitrite ( $\sim 50$ -fold) was added. The concentrations of the  $d_1\text{NO}$  of Y10F and wt were 0.5 and 0.32 mM, respectively. W-band measurements were carried out on a high-power home-built spectrometer.<sup>18</sup>

The cw X-band EPR spectra of wt and Y10F  $d_1\text{NO}$ , shown in Figure 1A, are similar in general, except for a small but detectable contribution from the axial form in Y10F. The wt  $d_1\text{NO}$  spectrum is similar to that reported earlier.<sup>9</sup> The W-band echo-detected EPR spectra are similar as well (Figure 1B), revealing the dominance of a species with rhombic  $g$  values,  $g_{xx}, g_{yy}, g_{zz} = 2.055, 1.96, \text{ and } 1.99$ , respectively. The W-band HYSCORE spectra recorded at different  $g$  values were also the same. As an example, Figures 2A,B present the spectra of wt and Y10F  $d_1\text{NO}$  recorded at  $g = 2.00$  and 1.99, respectively. The cross peaks are assigned to  $^{14}\text{N}(\text{His})$ .<sup>9</sup> Spectra of Y10F  $d_1\text{NO}$  recorded at  $g = 1.96$  and 2.055 (Figures 2C,D) show the same types of peaks of  $^{14}\text{N}(\text{His})$  (as in  $g = 1.99$ ). All frequencies observed are listed in Table S1. Additional cross peaks observed in the  $(-, +)$  quadrants at (26.6, 4.7) MHz were attributed to  $^{14}\text{NO}$  (Figure S1 in the Supporting Information).

We refer to the  $^{14}\text{N}$  frequencies in the  $\alpha, \beta$  electron-spin manifolds as  $\nu_{\text{sq}1}^{\alpha, \beta}$ ,  $\nu_{\text{sq}2}^{\alpha, \beta}$  and  $\nu_{\text{dq}}^{\alpha, \beta}$  corresponding to the single- and double-quantum transitions, respectively. Because this is the first application of HYSCORE at a high field, we have also carried out Davies ENDOR measurements on Y10F  $d_1\text{NO}$ , to substantiate the signal assignment. The spectra presented in Figure 3 show only the  $\nu_{\text{sq}1}^{\beta}$  and  $\nu_{\text{sq}2}^{\beta}$  lines of  $^{14}\text{N}(\text{His})$  because low-frequency signals are difficult to detect and double-quantum lines have very low transition probabilities in ENDOR. This highlights the advantages of W-band HYSCORE for this window of hyperfine couplings. The ENDOR spectra also show  $^{14}\text{N}$  signals of the NO and of the heme pyrrole. Some of these are not observed in the HYSCORE spectra. The ENDOR spectrum show only one type of pyrrole signal, although not all four are expected to be equivalent.<sup>23</sup>

Using the observed  $^{14}\text{N}$  frequencies, we have estimated the hyperfine and quadrupolar couplings from the first-order expressions of the ENDOR frequencies,  $\nu_{\text{sq}1,2}^{\alpha, \beta} = 0.5A \pm \nu_1 \pm 1.5Q$ , where  $A$  and  $Q$  are the hyperfine and quadrupole splittings. These values were then refined by simulations of both the ENDOR and HYSCORE spectra with the same parameters, focusing on peak positions (see Figures 2 and 3). There are small differences in line positions between the ENDOR and HYSCORE spectra and therefore there are small frequency differences between the calculated and experimental HYSCORE spectra. The simulations gave for  $^{14}\text{N}(\text{His})$  ( $A_{xx}, A_{yy}, A_{zz}$ ) =  $\pm(16.0, 19.5, 19.5) \pm 0.1$  MHz with Euler angles of  $(0, 0, 15)^\circ$  and ( $Q_{xx}, Q_{yy}, Q_{zz}$ ) =  $\pm(-0.45, -0.85, 1.3) \pm 0.1$  MHz with  $(0, 0, 70)^\circ$ . The Euler angles represent passive rotations that transform the  $\mathbf{A}$  matrix or the  $\mathbf{Q}$  tensor from their Eigenframe to the  $g$  Eigenframe ( $g_{xx}, g_{yy}, g_{zz}$ ). These results show that  $Q_{zz}$  is along  $g_{zz}$  and that the largest anisotropic hyperfine component is  $15^\circ$  of  $g_{xx}$  (see Figure S2 in the Supporting Information). For  $^{14}\text{NO}$ , ( $A_{xx}, A_{yy}, A_{zz}$ ) =  $\pm(33.5, 26.9, 64.5) \pm 0.2$  MHz and for  $^{14}\text{N}(\text{heme})$  ( $A_{xx}, A_{yy}, A_{zz}$ )  $\sim (3.3, 3.1, 2.5)$  MHz, ( $Q_{xx}, Q_{yy}, Q_{zz}$ )  $\sim (-0.36, -0.54, 0.9)$  MHz and  $(0, 50, 60)^\circ$ . The  $Q_{zz}$  value was taken from the literature.<sup>24</sup>

In principle, if the orientation of the  $^{14}\text{N}$  hyperfine and quadrupole tensor principal axes are known with respect to molecular parameters then the orientations we have obtained should provide the orientation of  $g$  with respect to the complex structure (and vice versa). Unfortunately, these relationships are not obvious, and some discussion on this issue is presented in the Supporting Information.

In summary, we have shown that Tyr10 has practically no effect on the structure of the NO complex in solution, in agreement with the crystal structure.<sup>11</sup> We demonstrated that W-band HYSCORE is an excellent tool for characterizing  $^{14}\text{N}$  nuclei with  $A \sim 20$  MHz for which,  $A \sim 2\nu_1$  ( $\nu_1$  is the  $^{14}\text{N}$  Larmor frequency). In addition to nitrosyl-heme com-

(13) Flores, M.; Wajnberg, E.; Bemski, G. *Biophys. J.* **2000**, *78*, 2107–2115.

(14) Tyryshkin, A. M.; Dikanov, S. A.; Reijerse, E. J.; Burgard, C.; Huttermann, J. *J. Am. Chem. Soc.* **1999**, *121*, 3396–3406.

(15) Parr, S. R.; Barber, D.; Greenwood, C.; Phillips, B. W.; Melling, J. *Biochem. J.* **1976**, *157*, 423–430.

(16) Silvestrini, M. C.; Cutruzzolà, F.; D'Alessandro, R.; Brunori, M.; Fochesato, N.; Zennaro, E. *Biochem. J.* **1992**, *285*, 661–666.

(17) Silvestrini, M. C.; Colosimo, A.; Brunori, M.; Walsh, T. A.; Barber, D.; Greenwood, C. *Biochem. J.* **1979**, *183*, 701–709.

(18) Goldfarb, D.; Lipkin, Y.; Potapov, A.; Gorodetsky, Y.; Epel, B.; Raitsimring, A. M.; Radoul, M.; Kaminker, I. *J. Magn. Reson.* **2008**, *194*, 8–15.

(19) Jeschke, G.; Rakhmatullin, R.; Schweiger, A. *J. Magn. Reson.* **1998**, *131*, 261–271.

(20) *Simbud*, <http://chem.arizona.edu/rss/epr/software.html>.

(21) Stoll, S.; Schweiger, A. *J. Magn. Reson.* **2006**, *178*, 42–55.

(22) KAZAN, [http://www.boep.specman4epr.com/kv\\_intro.html](http://www.boep.specman4epr.com/kv_intro.html).

(23) Gilbert, D. C.; Dikanov, S. A.; Doetschman, D. C.; Smeija, J. A. *Chem. Phys. Lett.* **1999**, *315*, 43–48.

(24) Gilbert, D. C.; Doetschman, D. *Chem. Phys.* **2001**, *269*, 125–135.

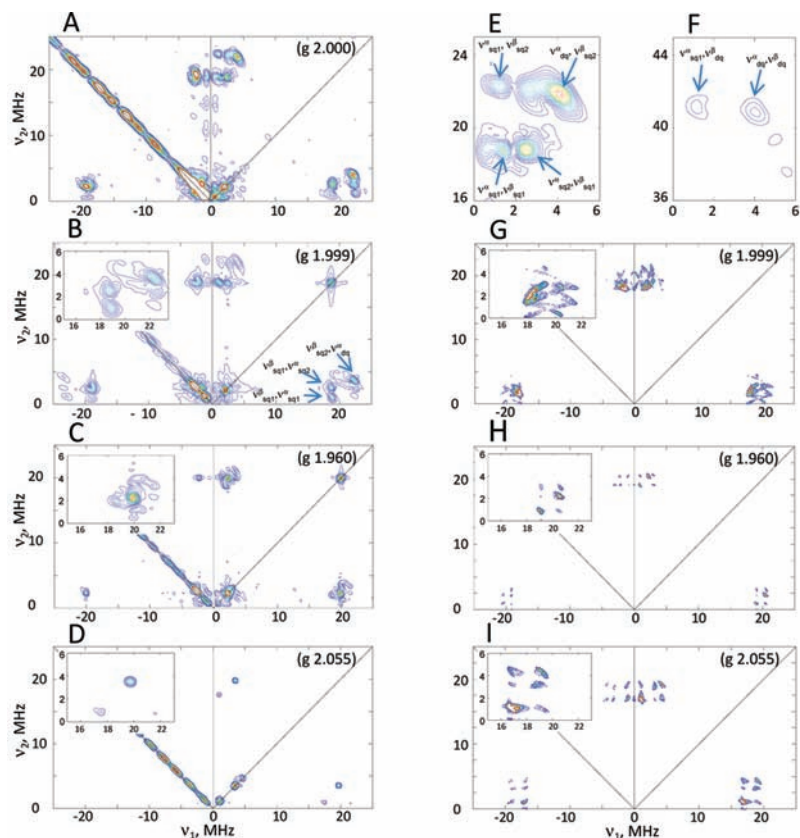


**Figure 2.** W-band-matched HYSORE<sup>19</sup> spectrum of wt d<sub>1</sub>NO (8 K) (A) (E and F show expanded regions) and W-band HYSORE of d<sub>1</sub>NO Y10F (B–D). The observer  $g$  values are noted on the figure. For wt, the  $\pi/2$ ,  $\pi$ , and matched pulse durations were 12.5, 25, and 25 ns, respectively. For Y10F, the  $\pi/2$  and  $\pi$  pulse durations were 16 and 32 ns, respectively. For all spectra  $\tau = 200$  ns. The peaks on the diagonal of the  $(-, +)$  quadrant are noise. G–I are the corresponding HYSORE simulations obtained with the program *Simbud*,<sup>20</sup> and the parameters are listed in the text. The insets are expanded spectral regions.

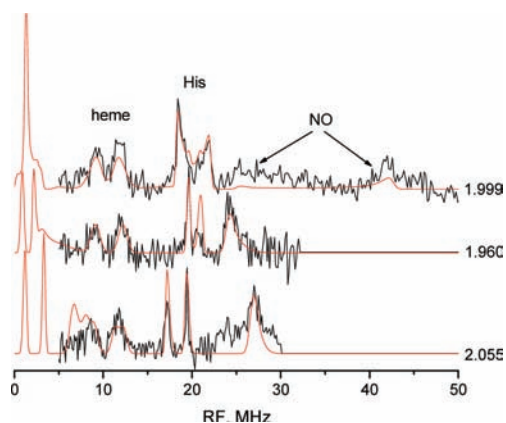


**Figure 3.** W-band Davies ENDOR spectra (7 K) of Y10F d<sub>1</sub>NO recorded at different  $g$  values. Experimental conditions: microwave pulses 200/100/200 ns, radio-frequency pulse 50  $\mu$ s. The solid lines are simulations obtained with parameters listed in the text using *Easyspin*<sup>21</sup> and *KAZAN*.<sup>22</sup>

plexes, it can be useful, for example, for copper(II) proteins with histidine ligands where  $A \sim 20\text{--}30$  MHz.<sup>25</sup> The

(25) Werst, M. M.; Davoust, C. E.; Hoffman, B. M. *J. Am. Chem. Soc.* **1991**, *113*, 1533–1538.

accumulation time of the W-band HYSORE spectra was significantly shorter than that of the ENDOR spectra, and for <sup>14</sup>N(His) the information content was richer.

The detailed characterization, in terms of spin-Hamiltonian parameters, of the rhombic form of d<sub>1</sub>NO in solution given here could be helpful for the future analysis of high-resolution EPR spectra of nitrosyl–heme complexes, which include both the axial and rhombic forms. This is an essential step toward understanding the factors that determine their presence.

**Acknowledgment.** This work was supported by the German–Israeli Science Foundation, the Binational USA–Israel Science Foundation, and the MIUR of Italy (Grant RBIN04PWN-002 to F.C.). D.G. holds the Erich Klieger Chair in Chemical Physics. We thank Dr. A. Astashkin for the *Simbud* program and Dr. B. Epel for the *KAZAN* software.

**Supporting Information Available:** Table with frequencies of cross peaks, a HYSORE spectrum showing <sup>14</sup>NO signals, the tensor orientations found and a brief discussion. This material is available free of charge via the Internet at <http://pubs.acs.org>.

IC802355Y